



Research paper

Development and evaluation of colloidal modified nanolipid carrier: Application to topical delivery of tacrolimus

Pallavi V. Pople, Kamalinder K. Singh *

C.U. Shah College of Pharmacy, S.N.D.T. Women's University, Mumbai, India

ARTICLE INFO

Article history:

Received 19 November 2010

Accepted in revised form 21 February 2011

Available online 3 April 2011

Keywords:

Modified carrier

Tacrolimus

Entrapment efficiency

Improved skin permeation

Skin localization

ABSTRACT

Low solubility of tacrolimus in carrier matrix and subsequent poor *in vivo* bioavailability was overcome by constructing modified nanolipid carrier (MNLC) as a novel approach. The aim of this study was to develop MNLC with enhanced drug solubility in carrier lipid matrix using lipophilic solubilizers for topical delivery. Comprehensive characterization of tacrolimus-loaded MNLC (T-MNLC) was carried out for particle size, morphology, and rheology. Lipid modification resulted in the formation of less perfect crystals offering space to accommodate the dissolved drug leading to high entrapment efficiency of 96.66%. Compatibility and mixing behavior of carrier constituents was evaluated using DSC, FT-IR, and ¹H NMR. T-MNLC displayed sufficient stability that could be attributed to possibility to reduce total lipid concentration in carrier. T-MNLC-enriched gels showed significantly higher *in vitro* drug release, skin permeation, and *in vivo* bioavailability with dermatopharmacokinetic approach in guinea pigs compared to commercial ointment, Protopic® as reference. Penetration-enhancing effect was confirmed using gamma scintigraphy *in vivo* in rats. Radioactivity remained localized in skin at the application site avoiding unnecessary biodisposition to other organs with prospective minimization of toxic effects. Skin irritation studies showed T-MNLC to be significantly less irritating than reference. Research work could be concluded as successful development of novel T-MNLC using lipophilic solubilizers to increase the encapsulation efficiency of colloidal lipid carriers with advantage of improved performance in terms of stability and skin localization.

© 2011 Elsevier B.V. All rights reserved.

1. Introduction

Tacrolimus, a metabolite of the fungus *Streptomyces tsukubensis*, is an anti-T-cell drug and acts by inhibiting the production of associated cytokines. It suppresses inflammation in a similar way to steroids, is equally as effective as a mid-potency steroid, and has been the object of considerable interest in the treatment of inflammatory conditions including atopic dermatitis (AD) [1]. Although it has shown notable efficacy, the most commonly observed side effects with its use are burning sensation and itching at the site of application. It has also been reported to have a potential to increase the risk of cutaneous infections by altering local cutaneous immune responses and can increase the severity as herpes zoster or polyoma viral infections. There are reports showing the incidences of producing lymphoproliferative disease upon sustained and prolonged exposure to tacrolimus [2,3]. Apart from having malignancy risk, it also has a

narrow therapeutic index and potential for serious drug interactions [4].

The drug has been marketed for the treatment of AD and other inflammatory skin conditions as topical ointment, Protopic® [5,6]. However, the overall adverse events' profile showed mild-to-moderate application site reactions, including skin burning, stinging, pruritus, and erythema [7,8]. Also the pharmacokinetic data showed low absorption of drug from the formulation [9,10,4]. All these factors demand the need for the development of novel carrier system which could effectively improve the skin penetration and reduce the undesirable side effects associated with the drug.

Various drugs require carriers for their delivery in an optimized way. The action or effect of the drug is governed not only by the properties of the drug but also by the carrier system [11]. The conventional drug delivery systems and methods of application are changing today paving the way for more and more products based on novel drug delivery systems with greater efficiency and effectiveness, better stability, lesser side effects, and toxicity with best patient compliance. Lipid-based colloidal drug delivery is the rapidly developing area and has contributed significantly to the advances in the field of targeted drug delivery. They are the focus of much attention due to their astonishing properties and numerous advantageous qualities for topical application. Particulate lipid

* Corresponding author. C.U. Shah College of Pharmacy, S.N.D.T. Women's University, Sir Vithaldas Vidyavihar, Juhu Road, Santacruz (West), Mumbai 400 049, India. Tel./fax: +91 22 26609577.

E-mail address: kksingh35@hotmail.com (K.K. Singh).

matrices in the form of lipid pellets are known since many years as the first generation of carriers [12]. Solid lipid nanoparticles (SLN) have been introduced at the beginning of the 1990s as a novel nanoparticulate delivery system produced from solid lipids, as an alternative carrier system to emulsions, liposomes, and polymeric nanoparticles [13,14]. They combine the advantages of other innovative carrier systems (e.g., physical stability, protection of incorporated sensitive drug molecules from degradation, controlled release, and excellent tolerability) while at the same time minimize the associated problems [15–17]. However, the drawbacks of SLN are inherent as a result of the crystalline state of the nanoparticles, and they are associated with potential problems such as risk of gelation, particle growth, limited drug-loading capacity, and possibility of drug leakage during storage caused by unexpected polymorphic transitions with lipid transforming to more perfect β -modification. The resultant perfection of the crystal leaves less space to accommodate drug molecules leading to drug expulsion [18].

These limitations are avoided or minimized by the new generation, the nanostructured lipid carriers (NLC). These NLCs comprise of blend of solid and liquid lipids. Due to their differences in structure, they cannot fit together very well to form perfect crystal, containing a lot of imperfections to accommodate drug in molecular form with the advantage of improved drug-loading capacity [19,20]. But at high oil concentrations, due to miscibility gap of the two lipids (solid lipid plus oil), phase separation may occur during the cooling phase leading to the precipitation of tiny oily nanocompartments. Therefore, it cannot be clearly said whether the oil molecules are present within the solid matrix or stick on its outer surface. Oil expulsion from the NLCs made of glyceryl behenate solid matrix has been reported even in case of low oil loading such as 2% w/w [21], and therefore, increasing the oil content up to 10% or more could lead to the formation of oily droplets sticking on solid lipid particles or may form spots or even incomplete films on the particle surface. It has also been reported that increasing the oil content lead to the formation of small lipid platelet-like structure [22]. Thus, the advantages of high incorporation rate and protection from aqueous environment may not be truly achieved with NLCs. However, both SLN and NLC possess numerous features advantageous for topical route of application [23,24]. It was the objective of this study to overcome the above-mentioned limitations by modifying the lipid matrix so as to enhance the drug solubility in the lipid carrier by mixing solid lipid with lipophilic solubilizers (having very good solubility for the drug), leading to the formation of the modified nanolipid carrier (MNL). The present work investigates the formation of MNL that contained the drug dissolved in the solubilizer nanopockets within the solid lipid particle matrix (i.e., drug/solubilizer/solid lipid/water – D/S/L/W system).

Tacrolimus BCS Class II drug [25] has solubility problems being insoluble in aqueous media as well as most of the commonly used vehicle/carrier excipients. The present study reports the screening of various solid lipids, liquid lipids/oils, and solubilizers commonly used for the preparation of lipid-based drug delivery systems. The solubilizer showing the highest solubility for the drug was selected for the incorporation of tacrolimus. The drug–solubilizer (D/S) blend was then mixed with the melted solid lipid (L) for inclusion of the (D/S) droplets in the solid lipid forming D/S/L system. This lipid phase was then emulsified in the water phase (D/S/L/W) using suitable surfactant system and homogenized with high-pressure homogenization technique creating lipid dispersions having lipid nanoparticles with drug dissolved completely in it. In this multiple D/S/L/W system, drug can be accommodated within the nanopockets of lipophilic solubilizer. Higher amounts of drug can be accommodated due to greater solubility of drug in the selected solubilizer. A comprehensive evaluation of this

modified colloidal lipid carrier was carried out with respect to particle size and its distribution, particle morphology, rheology, entrapment efficiency, and storage stability. The structure and mixing behavior of lipids in the inner core of these colloidal particles was characterized by differential scanning calorimetry (DSC), Fourier transform infrared spectroscopy (FT-IR), and proton nuclear magnetic resonance (^1H NMR) measurements. Drug release and skin penetration properties have been studied comparatively with the commercial ointment product Protopic[®] using Franz diffusion assembly. The enhancement in bioavailability was demonstrated *in vivo* using dermatopharmacokinetic (DPK) approach as per the Food and Drug Administration (FDA) Draft guidance 1998 [26] by stratum corneum (SC) tape stripping technique [27–29] using guinea pig as the animal model. The detailed information on penetration and deposition after single topical application of formulations has been made *in vivo* in albino rat by labeling the formulations with radioactive material $^{99\text{m}}\text{Tc}$, followed by subsequent evaluation using gamma scintigraphy imaging. The comparative assessment of the safety profile of the developed formulation was made using Draize skin irritation study in albino rabbit. All animal experiments complied with the standards set out in the guidelines, and the study protocols were approved by the Institutional Animal Ethics Committee prior to the commencement of the study.

2. Materials and methods

2.1. Materials

Tacrolimus was obtained as a kind gift from Panacea Biotech Ltd., Punjab, India. Glyceryl behenate, glyceryl palmitostearate, propylene glycol monocaprylate, polyglyceryl oleate, propylene glycol monolaurate, and oleoyl macrogolglycerides were procured from Gattefosse, Gennevilliers, France, while glyceryl trimyristate was from Sasol, Germany. Polysorbate 80 (Tween 80) and sorbitan monooleate (Arlacel 80) were supplied by Uniqema, Gouda, Netherlands, and Carbopol 980 was from Lubrizol Advanced Materials, Inc., USA. Stannous chloride dihydrate was purchased from Rankem RFCL Limited (New Delhi, India). $^{99\text{m}}\text{Tc}$ as the radioactive daughter of molybdenum-99 was obtained by column solvent extraction and was procured from Board of Radiation and Isotope Technology (B.R.I.T., Mumbai, India). All other chemicals and solvents used in the studies were of HPLC or analytical reagent grade and were purchased from S. D. Fine Chemicals, Mumbai, India.

2.2. Screening of components for tacrolimus solubility

Solubility of drug in the lipid phase is one of the most important factors that determine the loading capacity of the drug in the lipid carrier. Various solid lipids, liquid lipids, and lipophilic solubilizers were screened for the solubility of tacrolimus. Solid lipids such as glyceryl behenate, glyceryl palmitostearate, glyceryl trimyristate, hard paraffin, hard fat triglyceride ester, and lauroyl polyoxyglyceride were investigated. Liquid lipids and lipophilic solubilizers investigated were medium-chain triglycerides such as Miglyol 808 and Miglyol 812, oleoyl macrogolglycerides, propylene glycol monolaurate, polyglyceryl oleate, propylene glycol monocaprylate, polypropylene glycol (26) monooleate, PPG-26 oleate, and caprylocaproyl macrogolglycerides. Weighed quantity of tacrolimus was taken in series of test tubes, and different solubilizers in increasing amount were added. The test tubes were sonicated and observed for complete solubilization of drug. The solubility determination in solubilizers was carried out at room temperature. The results are compiled in Tables 1 and 2.

Table 1

Solubility of tacrolimus in solid lipids.

Solid lipid	Solubility ($\mu\text{g}/\text{mg}$)
Glyceryl behenate	35.76 ± 2.21
Glyceryl palmitostearate	26.95 ± 3.36
Glyceryl trimyristate	22.51 ± 3.17
Hard paraffin	Insoluble
Hard fat triglyceride ester	20.38 ± 1.54
Lauroyl polyoxyglyceride	30.05 ± 2.1

Table 2

Solubility of tacrolimus in various liquid lipid/lipophilic solubilizers.

Liquid lipid/lipophilic solubilizer	Solubility ($\mu\text{g}/\text{mg}$)
Miglyol 808	7.49 ± 5.63
Miglyol 812	5.92 ± 3.45
Oleoyl macroglycerides	Insoluble
Propylene glycol monolaurate	75.85 ± 9.8
Polyglyceryl oleate	Insoluble
Propylene glycol monocaprylate	113.06 ± 6.4
Polypropylene glycol (26) monooleate	Insoluble
PPG-26 oleate	Insoluble
Caprylocaproyl macroglycerides	30.90 ± 2.6

2.3. Formulation of modified nanolipid carrier (MNLC)

Tacrolimus-loaded MNLC (T-MNLC) system was prepared using following steps:

Step 1: Tacrolimus (0.1% w/w) was dissolved in the minimum amount of propylene glycol monocaprylate (0.5% w/w) as lipophilic solubilizer by slight warming leading to the formation of drug/solubilizer (D/S) phase.

Step 2: Glyceryl trimyristate (2% w/w) was melted (at 60 °C) and added to the above mixture giving drug/solubilizer/solid lipid (D/S/L) system.

Step 3: The D/S/L system was emulsified in the previously heated aqueous dispersion medium (70 °C) by high-speed stirring using Ultra-turrax T 25 (IKA-Werke, Staufen, Germany) forming drug/solubilizer/solid lipid/water (D/S/L/W) system.

Step 4: The above dispersion was then subjected to high-pressure homogenization using APV 2000 (Invensys, Copenhagen, Denmark) homogenizer.

The obtained nanodispersion was allowed to cool to room temperature forming a modified nanolipid carrier (MNLC).

2.4. Formulation of gels enriched with tacrolimus-loaded MNLC (T-MNLC)

In order to achieve a desired viscosity and texture for topical purposes, T-MNLC was processed to semisolid vehicle with adequate rheological characteristics. Carbopol 980 (0.5% w/w) was used as the gel-forming polymer and incorporated in T-MNLC dispersions to obtain the required consistency. Triethanolamine was used to neutralize the dispersions, and glycerol (5% w/w) was added in the gels as hydrating agent.

2.5. Particle size and polydispersity index (PI) measurements of T-MNLC dispersion

The measurements were taken using Beckmen N5 Submicron Particle Size Analyzer (Beckmen, Inc., USA) in triplicates, at a temperature of 20 °C under a fixed angle of 90° applying the principle

of photon correlation spectroscopy (PCS). Dispersions were diluted suitably. Double-distilled and filtered water (through 0.2- μ membrane filter) was used to dilute the samples, so as to ensure that the light-scattering intensity (between $5e+004$ and $1e+006$) was within the instrument's sensitivity range.

2.6. Transmission electron microscopy (TEM)

For TEM imaging, the copper grids having a thin layer of carbon were loaded with T-MNLC dispersion and allowed to dry under an IR-lamp. After the sample was dried thoroughly, the images were captured on a Philips CM200 Transmission Electron Microscope (Philips, Eindhoven Area, Netherlands) with 0.23 nm resolution and accelerating voltage of 200 kV.

2.7. Entrapment efficiency (EE)

The percentage of incorporated tacrolimus (entrapment efficiency) was determined by high-performance liquid chromatography (HPLC) determination at 210 nm, after the separation of free drug and the lipid material from the aqueous medium. Aqueous solution of tetrahydrofuran (30% w/w) was used for the aggregation of nanolipid carrier [30]. After centrifugation of the resultant dispersion, the amount of free drug in the supernatant was estimated. The amount of incorporated drug was determined as the difference between the initial drug content and the free drug in the supernatant.

2.8. Analysis of T-MNLC structural composition

2.8.1. Differential scanning calorimetry (DSC) measurements

The structure and mixing behavior of lipid constituents of T-MNLC particles was characterized by DSC using DSC Q200 TA instrument (New Castle, Delaware, USA). An empty standard aluminum pan was used as reference. The measurements were taken between 30 and 200 °C at a rate of 10.0 °C/min. The individual components of T-MNLC were also analyzed.

2.8.2. Fourier transform infrared (FT-IR) measurements

In order to certify the encapsulation of drug in the nanocarrier and interaction between the drug and MNLC excipients, FT-IR analysis was carried out using JASCO FTIR – 4100 type A instrument with TGS detector (MD, USA). T-MNLC was vacuum-dried to obtain the FT-IR spectra. T-MNLC with individual components was analyzed by the potassium bromide disk method over the scanning wavelength range of 4000–600 cm^{-1} .

2.8.3. Proton nuclear magnetic resonance (^1H NMR) measurements

Structural features of developed nanolipid carrier were analyzed by ^1H NMR spectroscopy using Oxford NMR AS 400 spectrometer (Oxford, UK) having superconducting magnet, operating at 400 MHz and 20 °C. Signals were obtained using deuterated water (for aqueous samples) or chloroform-D1 (for the measurement of lipid samples and the drug) added for field lock. Signal assignment in the ^1H NMR spectra was made as given in the literature [31,32].

2.9. Stability of T-MNLC

Stability studies of T-MNLC were carried out at four different storage conditions (viz. refrigeration, 25 ± 2 °C/60 \pm 5% RH, 30 ± 2 °C/65 \pm 5% RH, and 40 ± 2 °C/75 \pm 5% RH) as per ICH guidelines. The samples were withdrawn at the predetermined time intervals of 1, 2, 3, 6, and 12 months and evaluated for appearance, particle size, and PI.

2.10. Rheological analysis

2.10.1. Viscosity determination

Brookfield Rheocalc® V 32 Rheometer (Middleboro, USA) LV model was employed to determine the rheological properties of aqueous T-MNLC systems using CP40 spindle equipped with a cone and plate test geometry. Brookfield Rheocalc® 2.010 Application Software was used for data analysis.

Viscosity of T-MNLC-enriched gels was determined using Brookfield R/S-CPS Plus Rheometer (Middleboro, MA, USA), a rotational speed and stress-controlled Rheometer with spindle C25-2 DIN as the measuring unit, and cone–plate geometry. The shear rate was increased in ascending order from 0 to 100 D[1/s] (up curve) and then decreased from 100 to 0 D[1/s] (down curve) and the resulting shear stress [Pa] was measured. All measurements were made in triplicate after equilibrating the samples at 25 °C.

2.10.2. Spreadability

Spreadability measurements of T-MNLC-enriched gels were made in triplicate using a wooden block and glass slide apparatus. Weighed amount of sample under study was applied to the lower plate of apparatus to get a uniform layer of the formulation. A weight of 100 g was added to the pan, and the time in seconds required for the upper plate to travel across the length of the lower plate was noted. This time was indicative of the spreadability, i.e., the ease with which a formulation may spread on the skin [33].

2.11. In vitro drug release studies

The modified Franz diffusion cell assembly has been employed with cellulose nitrate membrane (0.1- μ m pore diameter, Whatman GmbH, Germany), soaked with isopropyl myristate to simulate the lipophilic properties of the SC [34]. The assembly was thermoregulated with a water jacket at 32 ± 0.5 °C. Weighed quantity (0.25 g) of formulation was applied to the donor compartment. Aliquots were withdrawn at predetermined time intervals and analyzed by HPLC at 210 nm over a period of 48 h. Commercial topical product of tacrolimus (Protopic®, 0.1%) was used as reference for comparison in this and all the successive studies.

2.12. In vitro skin permeation study through pig ear skin

Pig ears were obtained post-sacrifice from a local abattoir (Deonar, Mumbai, India), before the pig carcass was exposed to the normal high-temperature cleaning procedure. The subcutaneous fat tissue was removed, and hair present was trimmed carefully as short as possible using scissors without damaging or scratching the surface in order to ensure the integrity of the skin barrier. Excised skin was then carefully mounted on the diffusion cell, and 0.25 g of formulation was applied on the SC side facing into the donor compartment, while the dermal side faced downwards into the receptor compartment. Assurance was made that the skin was completely in contact with the receptor phase by eliminating any air bubbles. Receptor phase was stirred constantly throughout the experiment, and the temperature was maintained at 32 ± 0.5 °C. The receptor medium was sampled at periodic time intervals and analyzed for tacrolimus using HPLC. At the end of 48 h, the formulation remaining on the skin was collected carefully and quantified to determine the concentration of tacrolimus that remained unabsorbed on the skin surface. The amount of tacrolimus deposited within the skin was determined by extraction of the skin followed by quantification using HPLC at 210 nm.

2.13. In vivo skin penetration studies using dermatopharmacokinetic (DPK) approach in guinea pigs

For the purpose of this study, hair from the back of adult guinea pigs weighing 350–400 g was removed carefully using depilatory cream 24 h before the study. Areas of 2.25 cm² were marked on the dorsal trunk of the animals using a template. Weighed quantities (150 mg) of the test formulations were uniformly applied over the treatment area. After the required contact time, the patch was removed and excess formulation was gently removed using cotton swabs. The SC was removed by validated tape stripping procedure [26]. The tapes (Micropore Tape, 3M, St. Paul, Minnesota) with adhering corneocytes were then manually removed carefully by pulling using firm tension in a consistent manner. The first two strips were discarded due to potential drug remaining on the skin surface and strips 3–14 were collected. Once removed from the skin, tapes were collected and pooled and the drug was extracted and quantified using a validated HPLC method.

To get a clear picture of tacrolimus dermal penetration, the study was conducted till 48 h and samples were collected at 0, 3, 6, 12, 24, 30, and 48 h after the commencement of study. The sampling points 3, 6, 12, and 24 h were selected to determine the uptake; the 30 and 48 h were used to assess the elimination of drug from the skin. It was assumed that any drug not removed by the surface-cleaning procedure at the end of the treatment period eventually became bioavailable to the skin. The time to reach steady state, the uptake and elimination time points were selected from the pilot study employed to assess the information on study duration.

The DPK parameters were calculated using noncompartmental method of analysis. The area under the SC drug concentration vs. time profile (AUC) was calculated by trapezoidal method. Time to reach the maximum SC drug concentration (T_{max}) and peak/maximum SC concentration (C_{max}) were determined by direct observation of the SC drug concentration vs. time profiles. The relative bioavailability of developed nanolipid carrier as compared with the reference was calculated using the following formula:

$$\text{Relative bioavailability} = [\text{AUC}]_{\text{T-MNLC}} / [\text{AUC}]_{\text{Ref}}$$

where $[\text{AUC}]_{\text{T-MNLC}}$ is the area under the curve of developed nanolipid carrier T-MNLC and $[\text{AUC}]_{\text{Ref}}$ is the area under the curve of reference.

2.14. In vivo skin deposition and biodisposition studies using gamma scintigraphy in albino rats

Formulations were radiolabeled with Technetium-99m (^{99m}Tc) by direct labeling method using stannous chloride as reducing agent [35]. Pre-radiolabeling studies involving the optimization of radiolabeling parameters were performed as reported earlier [36,37]. Adult albino Wistar rats weighing between 200 and 250 g were selected for the study. The fur was removed from the dorsal area of the trunk of the animals 24 h before testing, with due care to avoid abrading the skin which may alter its permeation properties. Under anesthesia (with diethyl ether), tacrolimus formulations (0.1% w/w, 100 mg) were applied to the dorsal skin of the rat to an area of around 2 cm diameter with a stainless steel spatula and covered with an occlusive bandage. After application, the animals were housed in individual cages.

Information on localized radioactivity and drug biodisposition was obtained from *in vivo* imaging counts. Static whole-body gamma images were obtained at periodic time intervals of 0, 0.5, 1, 2, 4, 6, 8, 12, and 24 h using gamma-camera computer system (GE-Integra) on count mode with LEGP Collimator (Fig. 14).

To confirm the deposition of radioactivity in the skin, animals were sacrificed at 4, 8, and 24 h post-application of test

formulations using overdose of ether inhalation and the skin at the application site was excised and analyzed for radioactivity after surface decontamination using well-type γ -scintillation counter (IC 4702), avoiding contamination of other areas of the body. Radioactivity in whole blood, plasma, and major tissues (liver, kidneys, spleen, heart, lung, and muscle at the application site) was counted after 4, 8, and 24 h as described above to determine the biodisposition of drug.

2.15. Assessment of skin irritation

The comparative evaluation of skin irritation potential of T-MNLC-enriched gel with reference was carried out using Draize primary skin irritation test on albino rabbits [38,39]. White New Zealand rabbits weighing 2.5–3 kg were acclimatized for 7 days before the beginning of the study. The 0.5 g of formulation was applied to the hair-free intact as well as abraded skin. The skin was observed for any visible change such as erythema (redness) or edema (swelling) after 24 h and 72 h. Observations were made using the Draize scale and scored between 0 and 4 to grade erythema and edema indicating a range from no response to a severe response. Formalin was taken as positive control and plain gel was used as negative control. The scores for erythema and edema were totaled for intact and abraded skin for all rabbits at 24 and 72 h. The primary irritation index (PII) was calculated by dividing the sum of the scored reactions by 24 (2 scoring intervals multiplied by 2 test parameters multiplied by 6, the number of rabbits).

2.16. Data analysis

Results were expressed as mean \pm standard deviation (SD). Statistical comparisons of the experimental results were made by one-way analysis of variance (ANOVA) employing Tukey's multiple comparison post-test. *P* value of <0.05 was considered as statistically significant.

3. Results and discussion

3.1. Screening of components for tacrolimus solubility

Out of various solid lipids investigated (Table 1), hard paraffin showed least solubility for tacrolimus. Though glyceryl behenate and glyceryl palmitostearate showed reasonable solubility for tacrolimus, the formulations showed the aggregation of particles and subsequent expulsion of drug. Both hard fat triglyceride ester and lauroyl polyoxyglyceride showed good solubilizing capacity for tacrolimus; however, they are hygroscopic under high-temperature conditions and dissolve/disperse in water due to their high HLB values. This dispersible nature of these excipients could prevent the formation of a solid structure in the ultimate dispersion, which is a prerequisite for fabrication of this carrier system. Therefore, glyceryl trimyristate was preferred to make MNLC system as solid lipid matrix.

A prerequisite to obtain good entrapment efficiency is sufficiently high solubility of drug in the lipid phase. Owing to overall low solubility of tacrolimus in solid lipids, it requires high concentrations (5% w/w or more) of solid lipids to completely solubilize the drug [40]. High lipid concentrations may compromise the stability of the system due to aggregation of lipid nanoparticles [18]. Therefore, to increase the stability and reduce the concentration of solid lipid, it was decided to first dissolve the drug in a solubilizer having best solubilizing property for the same.

Among the lipophilic solubilizers screened, maximum solubility of tacrolimus was found in propylene glycol monocaprylate followed by propylene glycol monolaurate; however, medium-chain

triglycerides such as Miglyol 808 and 812 showed poor solubilizing capacity for the drug (Table 2). Out of the other lipophiles studied, oleoyl macroglycerides, polyglyceryl oleate, polypropylene glycol (26) monooleate, and PPG-26 oleate showed very poor solubility for tacrolimus. Thus, solubility studies helped to streamline the choice of excipients for MNLC formation, and glyceryl trimyristate and propylene glycol monocaprylate were selected as lipid and solubilizer, respectively, for the preparation of T-MNLC system.

3.2. Preparation of tacrolimus-loaded modified nanolipid carrier (T-MNLC)

With T-MNLC, the low solubility of tacrolimus in the carrier matrix was overcome by modifying the lipid matrix by incorporation of solubilizer as a novel approach. It was possible to reduce the total lipid concentration in the formulation to 2% w/w in case of T-MNLC as compared with 5% w/w used in the formulation of tacrolimus solid lipid nanoparticles [40]. Hot melt emulsification involving high-pressure homogenization technique was used to prepare T-MNLC system. The coarse lipid dispersion was formed on addition of the lipid phase to the aqueous phase which after homogenization gave translucent nanoparticulate dispersion. The T-MNLC was further processed to T-MNLC-enriched gels, a topically applicable formulation with desired semisolid consistency.

3.3. Particle size and polydispersity index (PI) measurements of T-MNLC dispersion

Particle size distribution of T-MNLC dispersion was found to be in the range of 20–150 nm and the mean particle size was estimated to be 59.5 nm with a PI of 0.31, indicating a narrow particle size distribution.

3.4. Transmission electron microscopy (TEM)

The nanocarrier formation and morphology of T-MNLC was further studied by TEM that confirmed the production of lipid nanoparticles (Fig. 1). The particle size data obtained with TEM were in agreement with PCS results. The inner phase constitutes the reservoir of the system which contains the drug imbedded in solubilizer nanopockets that are blended with the solid lipid. Moreover, findings of this study also suggested a spherical nature of T-MNLC particles in contrast to the platelet-like structure observed by Jores et al. for NLC system based on glyceryl behenate and medium-chain triglycerides [22].

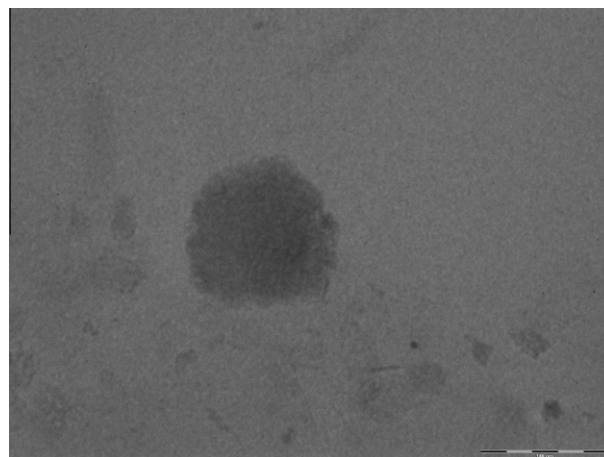


Fig. 1. The TEM imaging of T-MNLC.

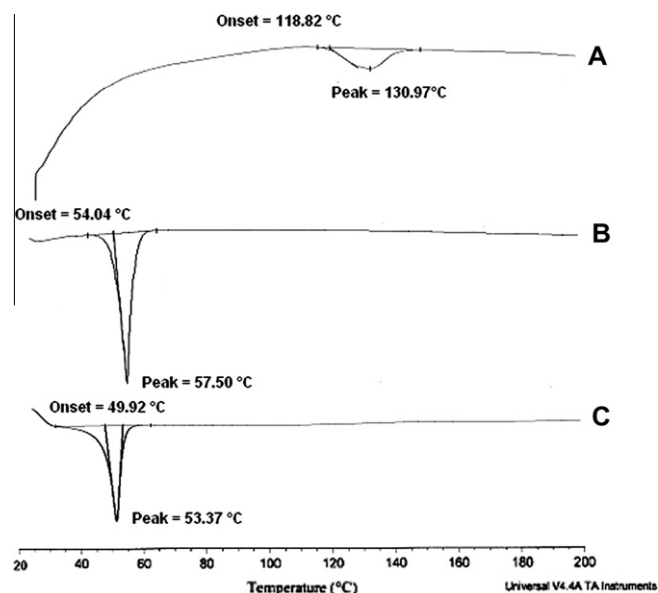


Fig. 2. DSC thermograms of pure tacrolimus (A), glyceryl trimyristate (B), and T-MNLC (C).

3.5. Entrapment efficiency (EE)

Tacrolimus at 0.1% w/w concentration could be successfully entrapped, equivalent to commercial Protopic® in the MNLC with high encapsulation efficiency of 96.66%. The lipids form highly crystalline particles, with a perfect lattice leading to drug expulsion [41]. On the other hand, the imperfection (lattice defects) of the lipid structure could offer space to accommodate the drug. Modification of lipid by incorporation of lipophilic solubilizer molecules might have resulted in the formation of less perfect crystals with many imperfections offering space to accommodate the dissolved drug. The minimum amount of solubilizer used (just required to dissolve the drug) might be responsible for complete immobilization of liquid nanodroplets of drug in the crystal imperfections of solid lipid avoiding ejection of the liquid lipid during the crystallization process at the cooling step. As the low solubility of tacrolimus in the carrier matrix was overcome by this approach, much lower quantity of lipid was required to get high EE.

3.6. Analysis of T-MNLC structural composition

3.6.1. Differential scanning calorimetry (DSC) measurements

The mixing behavior of solid lipid and lipophilic solubilizer in the T-MNLC was investigated by DSC [42,43]. It gave information about the melting, crystallization behavior, polymorphism, and crystal ordering of the solid and liquid constituents of the nanoparticles. Tacrolimus showed a melting endotherm at 130.97 °C (Fig. 2A). The thermal curve of glyceryl trimyristate bulk lipid showed endothermic peak at 57.50 °C (Fig. 2B). The melting endotherm of T-MNLC (Fig. 2C) showed complete absence of tacrolimus peak, indicating that tacrolimus was completely solubilized inside the lipid matrix of T-MNLC. DSC thermogram of T-MNLC showed endotherm with lower onset temperature (49.92 °C) and peak temperature (53.37 °C) values from those of the bulk lipid material.

Particle size distribution, particle shape, colloidal character, and particle environment have a big impact on the melting point. The decrease in melting temperature of nanoparticle compared with the bulk can be attributed to the small particle size and the incorporation of guest solubilizer molecules into the crystalline lattice

of the solid lipid leading to the formation of less ordered crystal. Thus, it could be concluded that the lipid as nanoparticles was in a less ordered arrangement as compared with the bulk material.

The mutual miscibility between the structurally different lipids with different chain length, i.e., mixing of lipophilic solubilizer (propylene glycol monocaprylate) and solid lipid (glyceryl trimyristate), would fix the solubilizer molecules in the crystal lattice of glyceryl trimyristate and prevent the relocation of the solubilizer molecules to form individual small lipophilic droplets. It seems likely that the solubilizer is completely incorporated in the matrix of the nanoparticles. This observation is in good agreement with the results obtained for mixed lipid SLN prepared from theobroma oil and goat fat [44].

Also since melting events of glyceryl trimyristate were detected, supercooled lipid particles can be excluded (in agreement with the NMR results of this study) as liquid and supercooled glyceride fractions cannot be registered with given experimental conditions.

3.6.2. Fourier transform infrared (FT-IR) measurements

FT-IR experiments were performed in order to further investigate the structural composition of T-MNLC, already observed by DSC. Typical FT-IR spectra of T-MNLC as well as those of bulk materials tacrolimus, glyceryl trimyristate, and propylene glycol monocaprylate are displayed in Fig. 3. Pure tacrolimus showed strong infrared absorption at 3446.17, 2935.13, and 1639.2 cm⁻¹. The presence of tacrolimus could not be identified in T-MNLC because of the clear absence of these peaks. More specifically, the infrared spectrum of T-MNLC showed peaks corresponding to its parent lipid constituents with peaks at 2800 and 1730 cm⁻¹ due to the —C—H alkanes and —C=O carbonyl ester group, respectively, of glyceryl trimyristate and propylene glycol monocaprylate. Similar observations have been reported by Viriyaroj et al. with Diazepam-glycerol behenate nanoparticles where IR spectra of SLN showed superimposition to its parent materials [45]. These results can be attributed to the complete encapsulation of the drug, tacrolimus. The results are in agreement with observations made by Lee et al. during their study on sunscreen agent encapsulated in SLN [30]. The authors observed similar absence of drug peaks in the bis-ethylhexyloxyphenolmethoxyphenyltriazine (BEMT)-loaded SLN, confirming that the matrix lipid cetyl palmitate successfully encapsulated the drug BEMT. An additional observation was that IR spectra of T-MNLC did not contain any new peak, suggesting no strong interaction and no incompatibility in the developed formulation.

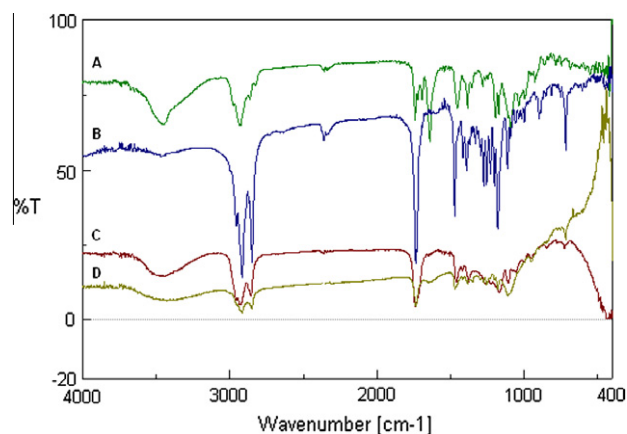


Fig. 3. FT-IR spectra of tacrolimus (A), glyceryl trimyristate (B), propylene glycol monocaprylate (C), and T-MNLC (D).

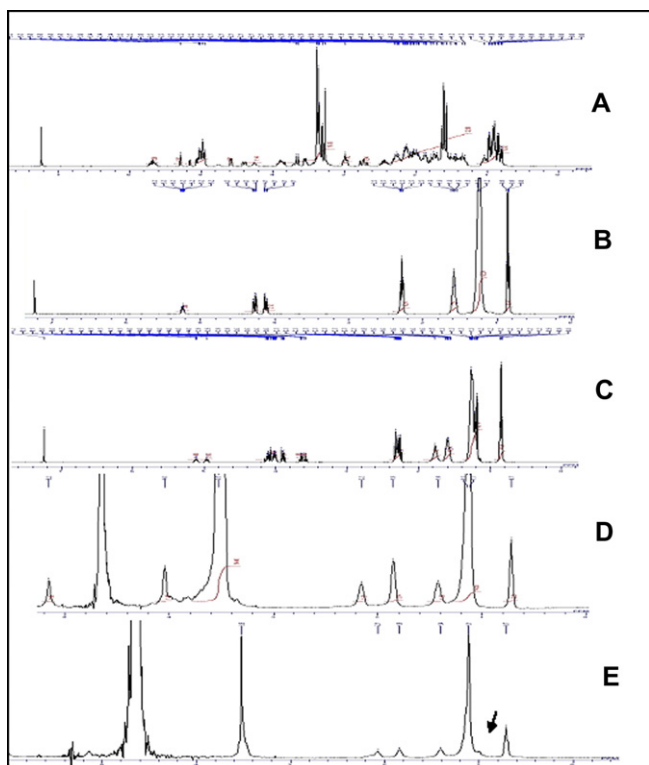


Fig. 4. Comparison of ^1H NMR spectra of T-MNLC with corresponding spectra of active ingredient tacrolimus (A), glyceryl trimyristate (B), propylene glycol monocaprylate (C), polysorbate 80 (D), and T-MNLC (E). The splitting of the signal is indicated by arrow. (For interpretation of the references to colour in this figure legend, the reader is referred to the web version of this article.)

3.6.3. Proton nuclear magnetic resonance (^1H NMR) measurements

^1H NMR is especially suited for the characterization of the liquid domains inside the solid colloidal particles [46]. The structure of the liquid (lipophilic solubilizer) inside the matrix of solid lipid was characterized by ^1H NMR measurements (Fig. 4). The information about the mobility and the arrangement of the liquid molecules is related to the chemical shift. Also the chemical shift of the signal results from the chemical neighborhood of the active nucleus. The parameter utilized in this study was chemical shift of the signals, which is related to the environment of the molecules.

The $-\text{CH}_3$ protons display signals at 0.9 ppm, while $-\text{CH}_2$ group exhibit signals at 1.25 ppm.

The closer a $-\text{CH}_2$ group is present to electronegative groups, the more the peaks are displaced to higher ppm values. The signals due to glycerol protons appear at around 4.0 ppm [46].

The peak assignment of the ingredients in the nanolipid carrier was facilitated by conducting ^1H NMR measurements of pure glyceryl trimyristate, propylene glycol monocaprylate, and polysorbate 80 as surfactant molecule. The methyl and methylene protons ($-\text{CH}_3$: 0.85 and $-\text{CH}_2$: 1.3) of the lipid show characteristic ppm values for alkyl fatty acid chains, while the protons present near or at the glycerol part of the lipid display higher ppm values. The ppm values for methyl and methylene groups of polysorbate 80 are shifted to lower ppm values as compared with the lipid protons and therefore can easily be distinguished from lipid signals. The ^1H NMR interpretation results for the assignment of the signals are in agreement with the literature [31,32].

The pure lipid can be characterized by intensive, clearly resolved, and sharp signals. In this study, two distinct chemical shifts for each of the fatty acid peaks were observed. The chemical shift values of the dominating peaks for the $-\text{CH}_3$ and $-\text{CH}_2$ protons of the fatty acids are demonstrated at 0.85 and 1.24–1.29 ppm.

For the $-\text{CH}_2$ protons next to the glycerol moiety ($\alpha\text{-CH}_2$), the chemical shift value was 2.29 ppm for the lipid and solubilizer molecules. However, the ^1H NMR spectra of T-MNLC showed chemical shifts of the peaks more close and corresponding to the surfactant molecules (Fig. 5). These observations are in agreement with the results reported by Jores et al. [21] for poloxamer-stabilized glyceryl behenate (GB) SLN, where only poloxamer-associated but no GB-derived signals were observed. These results further support the conclusion made in the DSC study that these colloidal particles are practically completely solid ruling out the phenomenon of supercooled melt, as the ^1H NMR signals corresponding to lipid protons are absent and solid materials are unable to give ^1H NMR signals under the given experimental conditions because of very short relaxation times.

Also broad peaks and loss of clear resolution of the observed signals of T-MNLC with splitting of the methylene signal at 1.1 ppm into two signals (shown by arrow) and the reduction of peak at 2.1 ppm for the $\alpha\text{-CH}_2$ protons to a peak shoulder can be attributed to decrease in proton relaxation times due to the higher rigidity of the interface (Fig. 4).

Tacrolimus did not produce any observable signal in the ^1H NMR spectra, suggesting complete encapsulation and immobilization of drug in the tiny nanocompartments of solubilizer inside the solid lipid matrix.

3.7. Stability of T-MNLC

The T-MNLC dispersion remained stable, with only a very slight change in particle size and PI values ($P > 0.05$) during the study period of 12 months at refrigeration condition suggesting good stability (Fig. 6). The increase in particle size at 25 °C/60% RH was from 59.53 to 74.8, 153.6, and 155.53 nm and the PI changed from 0.315 to 0.355, 0.378, and 0.454 at the end of 1, 2, and 3 months, respectively. The particle size remained lower than 300 nm during the 12-month study period. ANOVA showed that there were significant differences between the particle size values obtained at various time points ($P < 0.05$) at 30 °C/65% RH and 40 °C/75% RH. Mean particle size of T-MNLC stored at 30 °C/65% RH increased to 175, 408.6, and 627.6 nm at the end of 3, 6, and 12 months, respectively, with broader distribution. Though at 40 °C/75% RH, particle size of T-MNLC increased from 59.53 to 414.6 and 916.1 nm at the end of 6 and 12 months, respectively, it can be considered as significant improvement in stability as compared with our earlier report on tacrolimus lipid nanoparticles prepared using 5% lipid concentration where the particle size exceeded the 1 μm limit at the end of 6 months only [40]. As reported by Freitas and Muller, apart from storage temperature, lipid concentration has been found to be a significant factor affecting the stability of lipid nanoparticles [18]. The stability results obtained with T-MNLC are in agreement with Freitas and Muller with clear benefits of improvement in stability.

3.8. Rheological measurements

3.8.1. Viscosity determination of T-MNLC dispersions

As water is the major component of T-MNLC dispersions, it possessed a low viscosity of 0.90 cp and a yield value of practically zero (0.80). The flow curve displayed Newtonian flow characteristics as indicated by a straight line of shear rate vs. shear stress, passing through the origin (Fig. 7). It was observed that viscosity decreased with increasing shear stress, suggesting a nonfloculated system with very small particle size pointing toward the stability of the system. Therefore, T-MNLC dispersions were converted to a semisolid dosage form and characterized for its rheological properties concerning the particle size, and a comparison has been made with the plain gel base without having T-MNLC.

3.8.2. Viscosity determination of T-MNLC gels

The incorporation of T-MNLC into Carbopol 980 gels resulted in flow curves with pseudoplastic flow characteristics, with a decrease in viscosity observed with increasing rate of shear. Ascending and descending flow curves of the rheogram overlapped and showed no time effects like thixotropy. It could be hypothesized

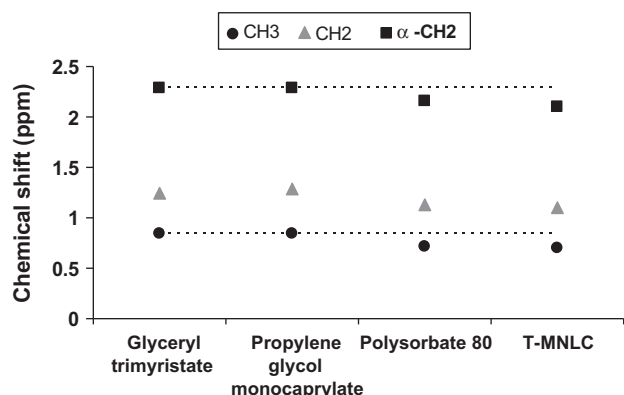


Fig. 5. Comparison of the chemical shifts (ppm) of the signals of T-MNLC with corresponding functional groups of the excipients. The dashed lines show the chemical shifts for —CH_3 and $\alpha\text{—CH}_2$ of the pure excipients.

that the T-MNLC particles in the semisolid system tend to align with increasing shear rate. This orientation might be responsible for reducing the internal resistance of the system. Smaller particle size of the dispersed system might also be the contributing factor to the observed low viscosity, which is apparent from the comparison of viscosity of T-MNLC-enriched gel with the plain semisolid gel (without any lipid particles) having almost similar viscosity (Figs. 8 and 9A). The greater mean size and the widest size distribution will preferentially show more viscous properties. The difference in the viscosities of the two systems studied was negligible with similar flow characteristics, suggesting no dependency of rheology upon the incorporated T-MNLC nanoparticles. Formulations showed optimum viscosity and consistency with easy application and smooth feeling when applied to the skin.

3.8.3. Spreadability

Spreadability values denote the ease of application of a topical dosage form on the skin. The spreadability data of T-MNLC-enriched gel were compared with the plain gel base without any lipid nanoparticles (Fig. 9B). The incorporation of T-MNLC nanoparticles did not affect the spreadability of plain gel base with almost similar spreadability values ($P > 0.05$). This observation could be attributed to the small particle size range and low PI values of T-MNLC nanoparticles giving low spreadability values indicating easy spreading on the skin.

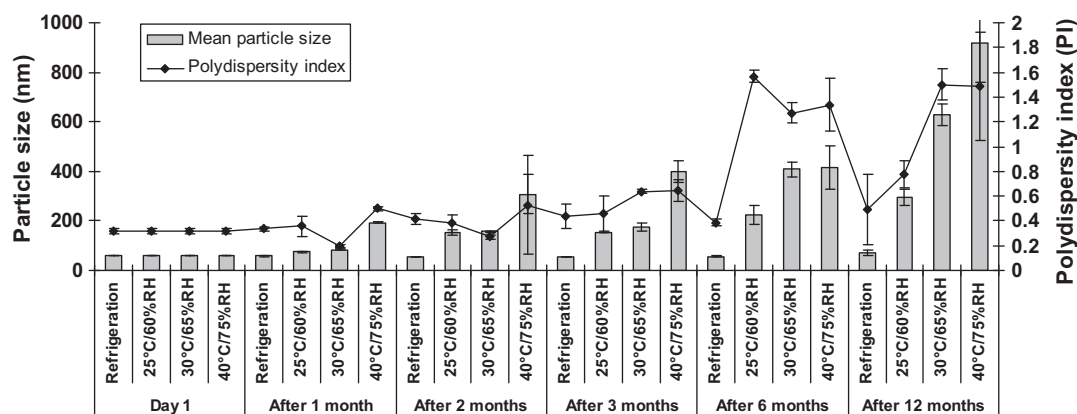


Fig. 6. Stability data of T-MNLC as per ICH guidelines indicating particle size (nm) and P.I. Data represent mean \pm SD, $n = 3$.

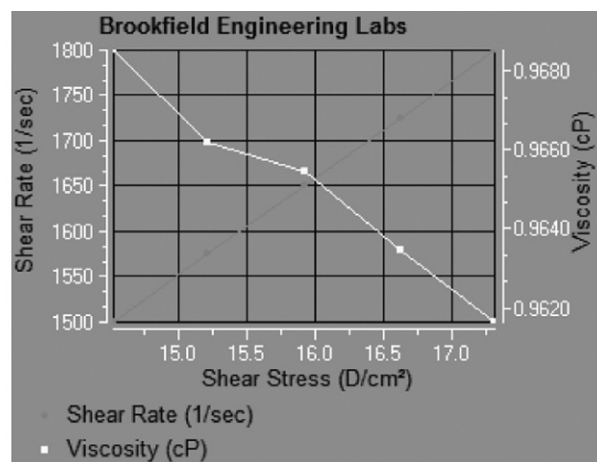
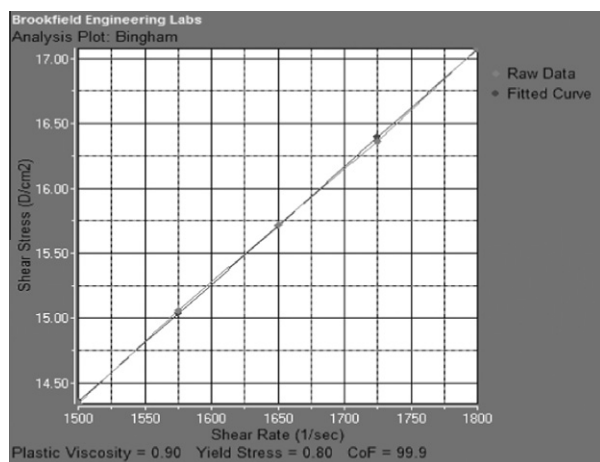


Fig. 7. Rheogram of T-MNLC dispersion showing correlation between shear stress and shear rate (A) and viscosity (B).

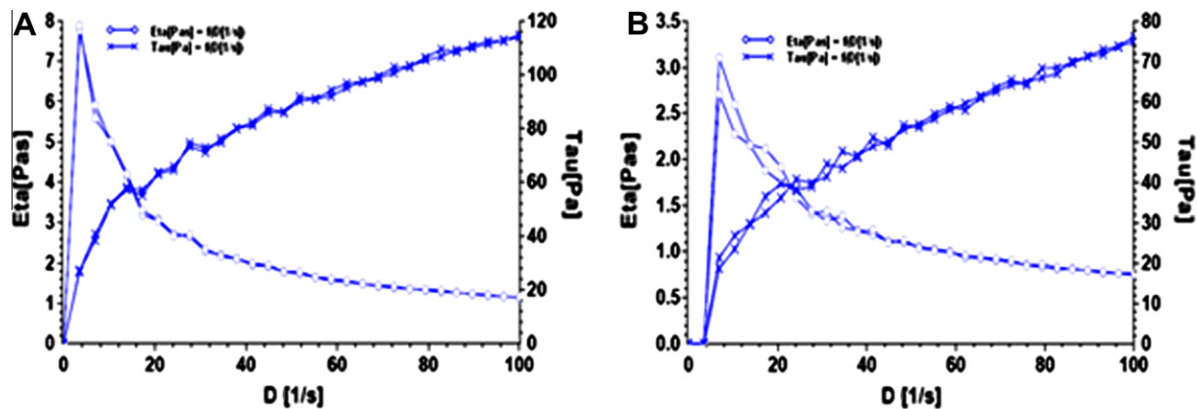


Fig. 8. Flow curves for gel enriched with T-MNLC (A) and plain gel base (B). (For interpretation of the references to colour in this figure legend, the reader is referred to the web version of this article.)

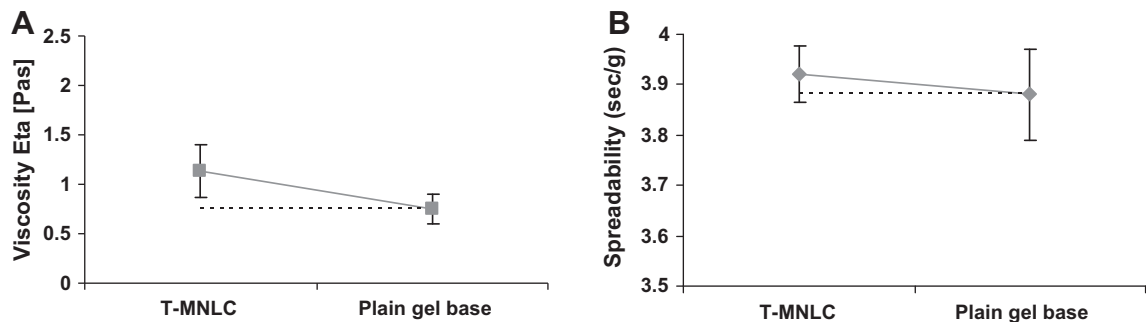


Fig. 9. Comparison of viscosity (A) and spreadability (B) values of T-MNLC with plain gel base.

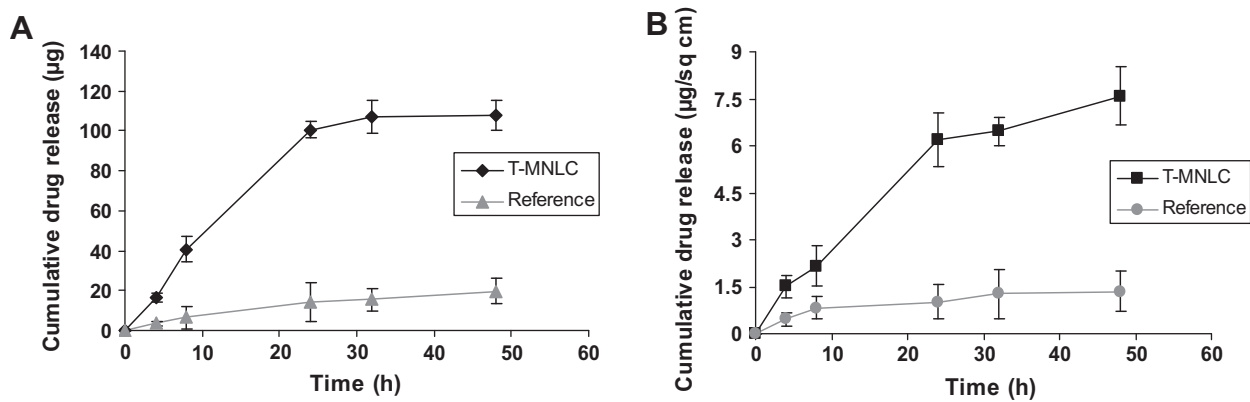


Fig. 10. Comparative *in vitro* drug release (A) and skin permeation profiles (B) of T-MNLC with reference.

3.9. *In vitro* drug release studies

In vitro drug release studies were carried out using both the developed T-MNLC-enriched gel and marketed conventional ointment product, Protopic® as reference, and the data were compared. T-MNLC-enriched gel showed a significantly faster and higher drug release ($P < 0.05$) at all the sampling times as compared with the reference (Fig. 10A). The release of tacrolimus from T-MNLC gels was almost 4.8–7.1 times higher when compared with reference.

The release kinetics of T-MNLC did not obey Higuchi equation as suggested by lower R^2 values, but a faster release occurred for first few hours indicating burst release pattern, after which the release

rate slowed down but it was much higher than the reference (Table 3). The tacrolimus release from reference followed Higuchi's equation indicating the release of drug from ointment matrix as a square root of time-dependent process based on Fickian diffusion.

Table 3
In vitro release kinetic parameters for gel enriched with T-MNLC and reference.

	Gels enriched with T-MNLC	Reference
R^2	0.9335	0.9856
<i>In vitro</i> release rate ($\mu\text{g}/\text{cm}^2/\text{h}^{1/2}$)	18.41	2.98

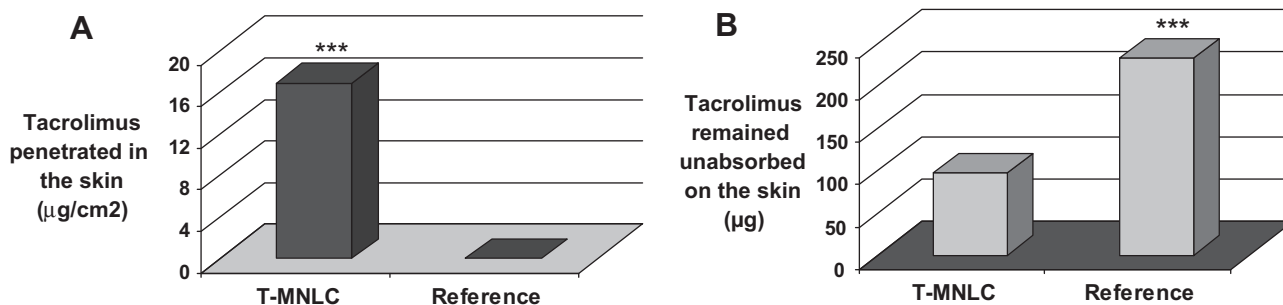


Fig. 11. Comparison of drug levels from *in vitro* skin penetration studies, penetrated in the skin (A) and remained unabsorbed on the skin (B).

3.10. *In vitro* skin permeation study through pig ear skin

The influence of vehicle on tacrolimus accumulation in and diffusion through the skin was evaluated using *in vitro* skin permeation studies. During this study, the permeation data of T-MNLC-enriched gel was compared with that obtained from reference ointment. T-MNLC-enriched gel displayed significantly higher permeation rate of tacrolimus at all the sampling times (almost 5.6- to 6.1-fold increased skin permeation of drug over reference), indicating an enhanced skin penetrating effect and localizing potential (Fig. 10B). Steady-state flux (J_{ss}) was determined from the quantity of drug permeated per square area vs. time profile. T-MNLC displayed a significantly higher J_{ss} value ($56.8 \pm 8.65 \text{ ng cm}^{-2} \text{ h}^{-1}$) when compared with the reference ($8.8 \pm 2.23 \text{ ng cm}^{-2} \text{ h}^{-1}$).

Skin deposition of tacrolimus in pig ear skin from T-MNLC was compared with the reference. There was a significant difference in the accumulative amount of tacrolimus between the two formulations. T-MNLC displayed significantly higher deposition of drug in the skin ($16.8853 \pm 3.74 \mu\text{g}/\text{cm}^2$). On the other hand, reference showed only a very small deposition of tacrolimus ($0.039 \pm 1.78 \mu\text{g}/\text{cm}^2$) in the skin (Fig. 11A).

The quantification of drug remaining unabsorbed at the end of 48 h showed almost 2.39-fold higher drug on the skin surface in case of reference as compared with the T-MNLC (Fig. 11B).

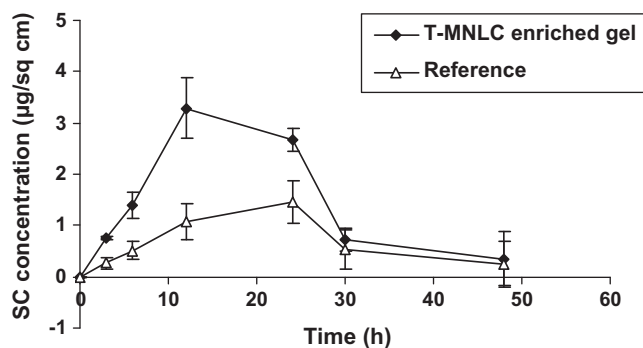


Fig. 12. SC concentration vs. time profiles of tacrolimus for gels enriched with T-MNLC and reference.

Table 4

DPK parameters for gel enriched with T-MNLC and reference according to noncompartmental analysis method.

Formulation	T_{\max} (h)	C_{\max} ($\mu\text{g}/\text{cm}^2$)	AUC_0^{48} ($\mu\text{g}/\text{cm}^2$)	AUC_0^{∞} ($\mu\text{g}/\text{cm}^2$)	F
T-MNLC gel	18	3.584	76.26 ± 23.51	86.84 ± 33.06	2.2
Reference	24	1.465	34.74 ± 15.78	76.25 ± 21.64	–

3.11. *In vivo* skin penetration studies using dermatopharmacokinetic approach in guinea pig

Fig. 12 shows the comparative DPK profiles for T-MNLC-enriched gel and reference, estimating the penetration and transfer rate of tacrolimus *in vivo* through the SC in guinea pigs. Application of one-way ANOVA with Tukey–Kramer multiple comparison tests showed the values of T_{\max} and C_{\max} to be significantly higher for T-MNLC-enriched gel as compared with the reference (Table 4) which indicated that tacrolimus could penetrate much more easily with T-MNLC than with ointment formulation. The AUC_0^{48} and AUC_0^{∞} values were lower for reference formulation than T-MNLC-enriched gel, and the relative bioavailability (F) of T-MNLC was 2.2 times higher than the reference. The better transport of drug through the SC barrier could be correlated with better bioavailability and would lead to greater therapeutic effect at the site of action. These results suggested improved efficiency with novel T-MNLC formulations than the conventional product.

3.12. *In vivo* skin deposition and biodisposition studies using gamma scintigraphy in albino rat

Tacrolimus formulations were radiolabeled with ^{99m}Tc . Pre-radiolabeling studies for the optimization of radiolabeling parameters such as SnCl_2 concentration and pH revealed that $100 \mu\text{g}$ of SnCl_2 at pH 7.0 produced maximum radiolabeling efficiency of 96.25 %. *In vitro* stability of the ^{99m}Tc -labeled complex was also tested, and the complex was found to be stable for up to 24 h.

Skin uptake and deposition was studied by sacrificing the animals at 4, 8, and 24 h. The applied radioactive formulation (as hot spot) was removed, and the area was decontaminated carefully. The radioactivity penetrated and remained localized in the application skin was quantified by measuring the activity in the excised application skin area (Fig. 13). Radioactivity in the carcass

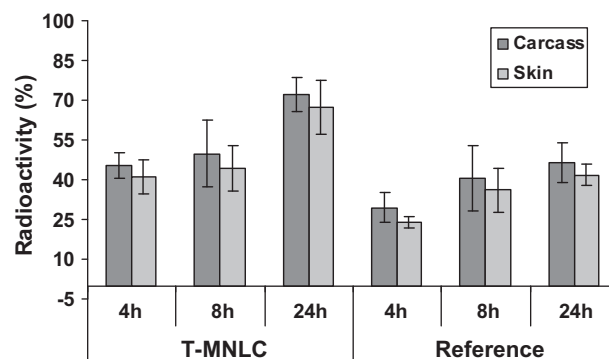


Fig. 13. Comparative evaluation of the radioactivity deposited in the skin as compared with the whole body.

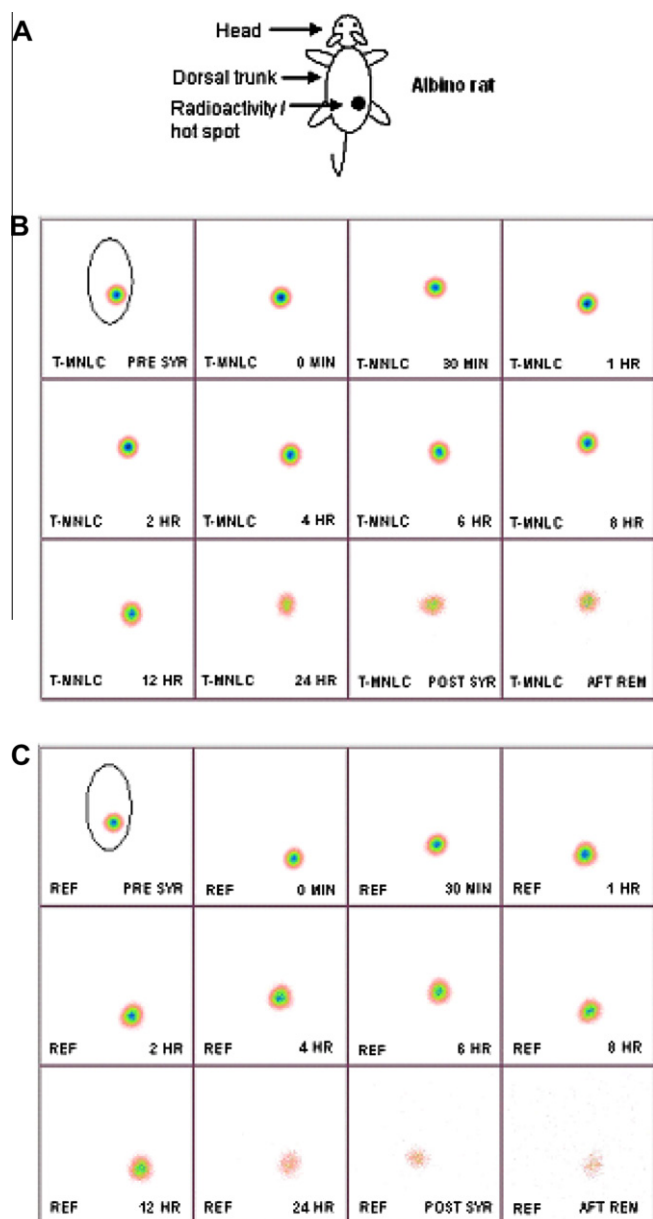


Fig. 14. Static whole-body images obtained after periodic time intervals up to 24 h of drug application. (Each scintigram is taken over a frame time of 60 s.) (A) Placement of radiolabeled formulations on the depilated dorsal trunk of albino rat; (B) T-MNLC-enriched gel and (C) reference. (For interpretation of the references to colour in this figure legend, the reader is referred to the web version of this article.)

was also measured. T-MNLC-enriched gel could penetrate very rapidly into the skin as significant activity was recorded in the skin (41.13%) after 4 h of application as compared with the reference (23.72%). The deposition of activity was much higher for T-MNLC than the reference throughout the study period of 24 h. These results suggested that encapsulation of tacrolimus in modified nanolipid carrier enhanced drug penetration and deposition in the skin. The results obtained here are in well accordance with previous findings of *in vivo* DPK study demonstrating increased penetration of drug when applied as T-MNLC system.

With topical drug delivery, specifically skin is targeted and the goal is to achieve maximum drug concentration in the skin with a minimum systemic uptake to avoid toxic effects. With this regard, the cumulative amount of drug reaching the systemic circulation is associated with potential toxicity with undesirable side effects

[29]. To observe for this effect, tissue distribution was studied to measure the unwanted spreading of activity to other organs of the body. This was performed by whole-body imaging at specific time points of 0, 0.5, 1, 2, 4, 6, 8, 12, and 24 h using gamma camera. The observation of the acquired gamma camera images showed the localization of radioactivity in the skin (visible as hot spot in the scintigrams) over the study duration of 24 h without any unnecessary spreading to other areas/organs of the body (Fig. 14). In addition to this, the rats were dissected at 4, 8, and 24 h and an attempt was made to estimate the radioactivity in blood, plasma, and other organs of the body (liver, kidneys, spleen, heart, lung, and muscle at the application site). The activity in blood, plasma, and various organs was also negligible (below the detection limit). The activity remained localized in the skin at the application site avoiding unnecessary biodisposition to other organs of the body with the prospective minimization of drug-related toxic effects.

Thus although the drug penetration and localization was significantly high with T-MNLC, only negligible amount of drug went into systemic circulation which confirmed the advantages of T-MNLC over reference formulation.

3.13. Assessment of skin irritation

The most common side effects associated with tacrolimus use are burning sensation and pruritus at the site of application. This strongly limits its utility and acceptability by the patients. Therefore, the delivery system of tacrolimus should be able to avoid or minimize these erythematic reactions. The results of skin irritation study showed no irritation symptoms such as erythema (redness) and edema (swelling) during 72 h after application, and all the scores were zero for T-MNLC-enriched gel (Fig. 15). The reference ointment triggered itching at the abraded application site, resulting in moderate skin irritation with PII calculated to be 3.33. The probable reason for the observed safety with T-MNLC could be the proper entrapment of tacrolimus in nanolipid carrier which avoided direct contact of drug with the skin, abolishing drug-related side effects. Thus, the formulation can be classified as a non-irritant to the rabbit skin.

4. Conclusion

The smart MNLC carrier would offer much more opportunity to load drugs with formulation-related issues such as poor solubility with advantages of enhanced effectiveness. It allows remarkable flexibility in drug loading, modulation of drug release, and improved performance in producing final dosage forms such as gels for topical application with excellent spreadability, appropriate viscosity, and skin feel at the same time avoiding the undesirable qualities such as greasiness and stickiness of the currently marketed products. Prolonged and controlled drug release with main effect to improve skin penetration through the barrier, i.e., SC and improved deposition at the target site, i.e., skin, would be advantageous over commercially marketed product and would be highly beneficial and more appealing with better patient compliance. Modified nanolipid carrier involving the use of lipophilic solubilizers to increase the solubility of drugs could be a new, effective, and interesting alternative to the currently available marketed products.

Conflict of interest

This research work is original and novel and all authors have read and approved the text and consent to its publication. There is no conflict of interest.

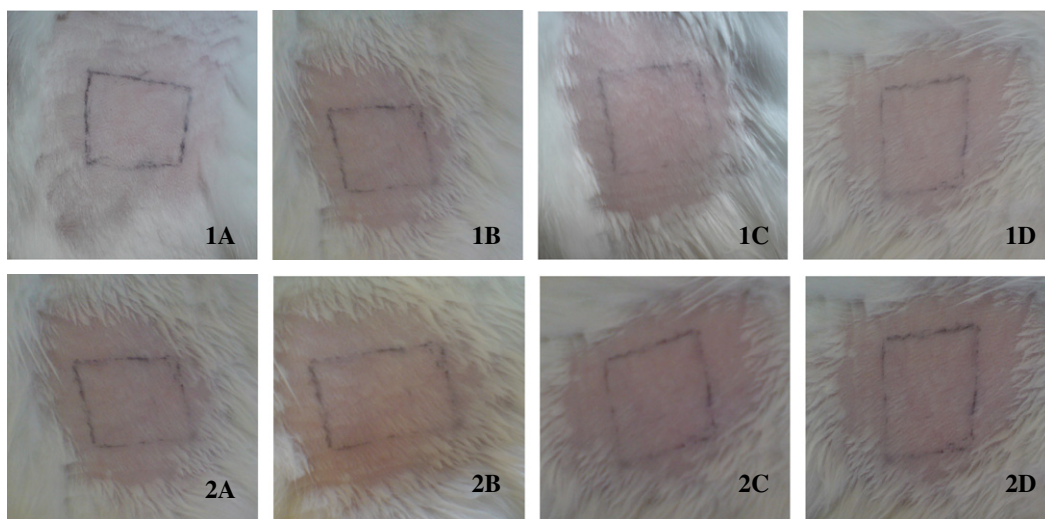


Fig. 15. Primary skin irritation photographs of rabbit skin; 1 denotes skin treated with T-MNLC and 2: reference; intact (A) and abraded (B) after 24 h; intact (C) and abraded (D) after 72 h. (For interpretation of the references to colour in this figure legend, the reader is referred to the web version of this article.)

Acknowledgements

We would like to acknowledge Gattefosse, France; SASOL Germany GmbH, Germany for the gift samples of lipid excipients. The authors are also thankful to Dr. Samad and Dr. Gaikwad from Department of Medicine, Bombay Veterinary College, Parel, Mumbai 400 012, India, for their help in carrying out the radiolabeling, skin deposition, and biodisposition studies.

References

- [1] T. Yamamoto, K. Nishioka, Topical tacrolimus: an effective therapy for facial psoriasis, *Eur. J. Dermatol.* 13 (2003) 471–473.
- [2] R.M. Wijnen, B.G. Ericzon, A.T. Tiebosch, W.A. Buurman, C.G. Groth, G. Kootstra, Toxicology of FK506 in the cynomolgus monkey: a clinical, biochemical, and histopathological study, *Transpl. Int.* 5 (Suppl. 1) (1992) S454–S458.
- [3] T. Hultsch, A. Kapp, J. Spergel, Immunomodulation and safety of topical calcineurin inhibitors for the treatment of atopic dermatitis, *Dermatology* 211 (2) (2005) 174–187.
- [4] H. Zahir, R.A. Nand, K.F. Brown, B.N. Tattam, A.J. Mclachlan, Validation of methods to study the distribution and protein binding of tacrolimus in human blood, *J. Pharmacol. Toxicol. Methods* 46 (1) (2001) 27–35.
- [5] T. Ruzicka, T. Assmann, B. Homey, Tacrolimus the drug for the turn of the millennium?, *Arch. Dermatol.* 135 (1999) 574–580.
- [6] H. Yoshida, S. Tamura, T. Toyoda, K. Kado, N. Ohnishi, R. Ibuki, In vitro release of tacrolimus from tacrolimus ointment and its speculated mechanism, *Int. J. Pharm.* 270 (2004) 55–64.
- [7] A. Rubins, R. Gutmane, N. Valdmann, P. Stevenson, C. Foster, N. Undre, Pharmacokinetics of 0.1% Tacrolimus ointment after first and repeated application to adults with moderate to severe atopic dermatitis, *J. Invest. Dermatol.* 125 (2005) 68–71.
- [8] D. Choi, H. Cho, Effect of tacrolimus derivatives on immunosuppression, *Arch. Pharm. Res.* 32 (4) (2009) 549–557.
- [9] T. Ruzicka, T. Bieber, E. Schopf, A short-term trial of tacrolimus ointment for atopic dermatitis, *N. Engl. J. Med.* 337 (1997) 816–821.
- [10] M. Boguniewicz, V.C. Fiedler, S. Raimer, A randomized vehicle-controlled trial of tacrolimus ointment for the treatment of atopic dermatitis in children, *J. Allergy Clin. Immunol.* 102 (1998) 637–644.
- [11] V.P. Torchilin, Multifunctional nanocarriers, *Adv. Drug Deliv. Rev.* 58 (2006) 1532–1555.
- [12] R.H. Muller, K. Mader, S. Gohla, Solid lipid nanoparticles (SLN) for controlled drug delivery – a review of the state of the art, *Eur. J. Pharm. Biopharm.* 50 (2000) 161–177.
- [13] E.B. Souto, S.A. Wissing, C.M. Barbosa, R.H. Müller, Development of a controlled release formulation based on SLN and NLC for topical clotrimazole delivery, *Int. J. Pharm.* 278 (2004) 71–77.
- [14] R.H. Müller, Lipid nanoparticles: recent advances, *Adv. Drug Deliv. Rev.* 59 (2007) 375–376.
- [15] A. Mühlén, C. Schwarz, W. Mehnert, Solid lipid nanoparticles (SLN) for controlled drug delivery – drug release and release mechanism, *Eur. J. Pharm. Biopharm.* 45 (2) (1998) 149–155.
- [16] J. Liu, W. Hu, H. Chen, Q. Ni, H. Xu, A. Yang, Isotretinoin-loaded solid lipid nanoparticles with skin targeting for topical delivery, *Int. J. Pharm.* 328 (2007) 191–195.
- [17] A. Nagi, A.L. Haj, R. Abdullah, S. Ibrahim, A. Bustamam, Tamoxifen drug loading solid lipid nanoparticles prepared by hot high pressure homogenization techniques, *Am. J. Pharmacol. Toxicol.* 3 (3) (2008) 219–224.
- [18] C. Freitas, R.H. Müller, Correlation between long-term stability of solid lipid nanoparticles (SLNs) and crystallinity of the lipid phase, *Eur. J. Pharm. Biopharm.* 47 (1999) 125–132.
- [19] R.H. Müller, M. Radtke, S.A. Wissing, Nanostructured lipid matrices for improved microencapsulation of drugs, *Int. J. Pharm.* 242 (2002) 121–128.
- [20] E.B. Souto, R.H. Müller, Investigation of the factors influencing the incorporation of clotrimazole in SLN and NLC prepared by hot high-pressure homogenization, *J. Microencapsul.* 23 (4) (2006) 377–388.
- [21] K. Jores, W. Mehnert, K. Mader, Physicochemical investigations on solid lipid nanoparticles and on oil-loaded solid lipid nanoparticles: a nuclear magnetic resonance and electron spin resonance study, *Pharm. Res.* 20 (8) (2003) 1274–1283.
- [22] K. Jores, W. Mehnert, M. Drechsler, H. Bunjes, C. Johann, K. Mader, Investigations on the structure of solid lipid nanoparticles (SLN) and oil-loaded solid lipid nanoparticles by photon correlation spectroscopy, field-flow fractionation and transmission electron microscopy, *J. Controlled Release* 95 (2004) 217–227.
- [23] M. Schäfer-Korting, W. Mehnert, H. Korting, Lipid nanoparticles for improved topical application of drugs for skin diseases, *Adv. Drug Deliv. Rev.* 59 (6) (2007) 427–443.
- [24] E.B. Souto, R.H. Müller, Cosmetic features and applications of lipid nanoparticles (SLN®, NLC®), *Int. J. Cosmet. Sci.* 30 (2008) 157–165.
- [25] S. Tamura, A. Ohike, R. Ibuki, G.L. Amidon, S. Yamashita, Tacrolimus is a class II low-solubility high-permeability drug: the effect of P-glycoprotein efflux on regional permeability of tacrolimus in rats, *J. Pharm. Sci.* 91 (3) (2002) 719–729.
- [26] V.P. Shah, Guidance for industry – topical dermatological drug product NDAs and ANDAs – in vivo bioavailability, bioequivalence, in vitro release and associated studies, US Dept. of Health and Human Services, Rockville (1998) 1–19.
- [27] A. Rougier, D. Dupuis, C. Lotte, R. Roguet, H. Schaefer, In vivo correlation between stratum corneum reservoir function and percutaneous absorption, *J. Invest. Dermatol.* 81 (1983) 275–278.
- [28] T. Kakuji, C. Aeri, M.S. Lee, A method for predicting steady-state rate of skin penetration in vivo, *J. Invest. Dermatol.* 92 (1989) 105–108.
- [29] C. Herkenne, I. Alberti, A. Naik, Y.N. Kalia, F. Mathy, V. Preat, R.H. Guy, In vivo methods for the assessment of topical drug bioavailability, *Pharm. Res.* 25 (1) (2008) 87–103.
- [30] G. Lee, D. Lee, K. Kang, C. Lee, H. Pyo, T. Choi, Preparation and characterization of bis-ethylhexyloxyphenolmethoxyphenyltriazine (BEMT) loaded solid lipid nano-particles (SLN), *J. Ind. Eng. Chem.* 13 (7) (2007) 1180–1187.
- [31] A.H. Beckett, J.B. Stenlake, Nuclear magnetic resonance spectroscopy, in: *Practical Pharmaceutical Chemistry*, fourth ed., Part two, Athlone Press, UK, 1988, pp. 408–467.
- [32] R.T. Morrison, R.N. Boyd, Spectroscopy and structure, in: *Organic Chemistry*, sixth ed., Prentice-Hall, Inc., 1992, pp. 585–655.
- [33] S. Honary, M. Chaigani, A. Majidian, The effect of particle properties on the semisolid spreadability of pharmaceutical pastes, *Indian J. Pharm. Sci.* 69 (3) (2007) 423–426.

- [34] V. Jennings, M. Schäfer-Korting, S. Gohla, Vitamin A-loaded solid lipid nanoparticles for topical use: drug release properties, *J. Controlled Release* 66 (2000) 115–126.
- [35] L.H. Reddy, R.K. Sharma, K. Chuttani, A.K. Mishra, R.R. Murthy, Etoposide-incorporated tripalmitin nanoparticles with different surface charge: formulation, characterization, radiolabeling, and biodistribution studies, *AAPS J.* 6 (3) (2004) (Article 23).
- [36] N. Subramanian, N. Arulsudar, K. Chuttani, P. Mishra, R. Sharma, R.S.R. Murthy, Radiolabeling, biodistribution and tumor imaging of stealth liposomes containing methotrexate, *Alasbimn J.* 6 (22) (2003) (Article No. AJ22-6).
- [37] N. Arulsudar, N. Subramanian, P. Mishra, K. Chuttani, R.K. Sharma, R.S.R. Murthy, Preparation, characterization, and biodistribution study of technetium-99m-labeled leuprolide acetate-loaded liposomes in ehrlich ascites tumor-bearing mice, *AAPS PharmSci.* 6 (1) (2004). Article 5.
- [38] J. Draize, G. Woodard, H. Calvery, Methods for the study of irritation and toxicity of substances applied topically to the skin and mucous membranes, *J. Pharmacol. Exp. Ther.* 82 (1944) 377–390.
- [39] P.V. Pople, K.K. Singh, Development and evaluation of topical formulation containing solid lipid nanoparticles of vitamin A, *AAPS PharmSciTech.* 7 (4) (2006) (Article 91).
- [40] P.V. Pople, K.K. Singh, Targeting tacrolimus to deeper layers of skin with improved safety for treatment of atopic dermatitis, *Int. J. Pharm.* 398 (2010) 165–178.
- [41] K. Westesen, H. Bunjes, M.H.J. Koch, Physicochemical characterization of lipid nanoparticles and evaluation of their drug loading capacity and sustained release potential, *J. Controlled Release* 48 (1997) 223–236.
- [42] H. Bunjes, K. Westesen, M.H.J. Koch, Crystallization tendency and polymorphic transitions in triglyceride nanoparticles, *Int. J. Pharm.* 129 (1996) 159–173.
- [43] D. Hou, C. Xie, K. Huang, C. Zhu, The production and characteristics of solid lipid nanoparticles (SLNs), *Biomaterials* 24 (2003) 1781–1785.
- [44] A.A. Attama, B.C. Schicke, T. Paepenmuller, C.C. Muller-Goymann, Solid lipid nanodispersions containing mixed lipid core and a polar heterolipid: characterization, *Eur. J. Pharm. Biopharm.* 67 (2007) 48–57.
- [45] A. Viriyaroj, G. Ritthidej, Diazepam-glycerol behenate nanoparticles for parenteral delivery prepared by the hot homogenization process, *Asian J. Pharm. Sci.* 1 (2006) 17–30.
- [46] V. Jennings, K. Mäder, S.H. Gohla, Solid lipid nanoparticles (SLN™) based on binary mixtures of liquid and solid lipids: a ¹H-NMR study, *Int. J. Pharm.* 205 (2000) 15–21.